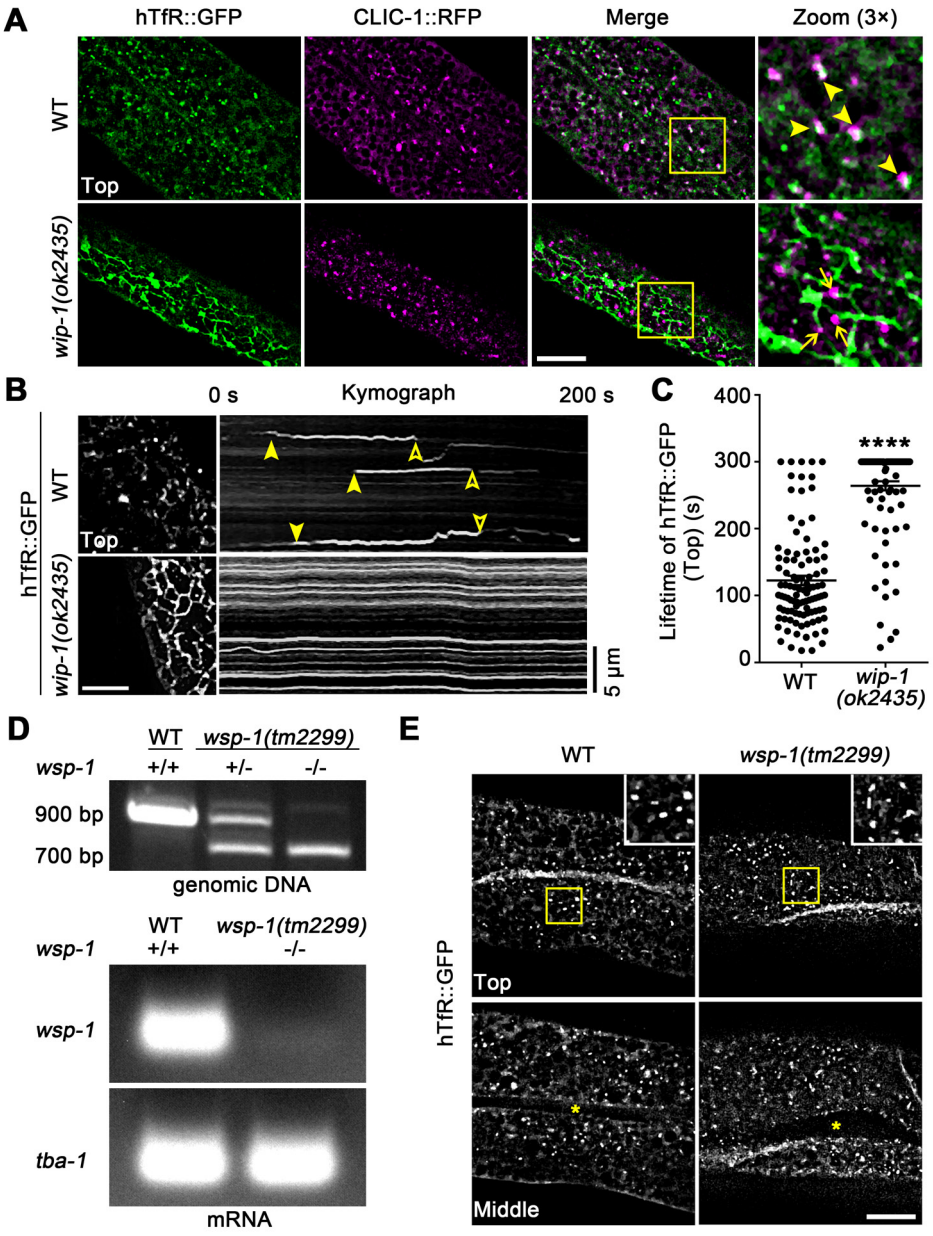

Fig. S1. WIP-1 function in CME in the *C. elegans* intestine is independent of WSP-1. (A) Colocalization images of hTfR::GFP with CLIC-1::RFP at the basal membrane in wild-type and *wip-1(ok2435)* mutant intestines. Insets show the enlargement of the indicated areas. Arrowheads point to positive overlap. Arrows indicate hTfR::GFP-tubules capped by CLIC-1::RFP upon loss of WIP-1. (B) Snapshots (Left) and kymographs (Right) of the representative time series from the basal membrane of the indicated intestines. Moments of hTfR::GFP appearance and disappearance are

marked by arrowheads. (C) Plots of individual lifetimes of hTfR::GFP from different intestines in wild-type and *wip-1(ok2435)* mutants, measured on dataset similar to B. *n*=100 events from 5 animals for each genotype. Data (mean±s.e.m.) were from three independent experiments in duplicate. ****P<0.0001 (Mann-Whitney). (D) PCR amplification of the targeted region using genomic DNA (Upper) or cDNA (Lower) extracted from each indicated genotype. (E) Representative confocal images show detailed distribution and architectures for intestinal hTfR::GFP signals in wild-type and *wsp-1(tm2299)* homozygotes. Asterisks depict the intestine lumen. Scale bars: 10 μm (A and E); 5 μm (B).

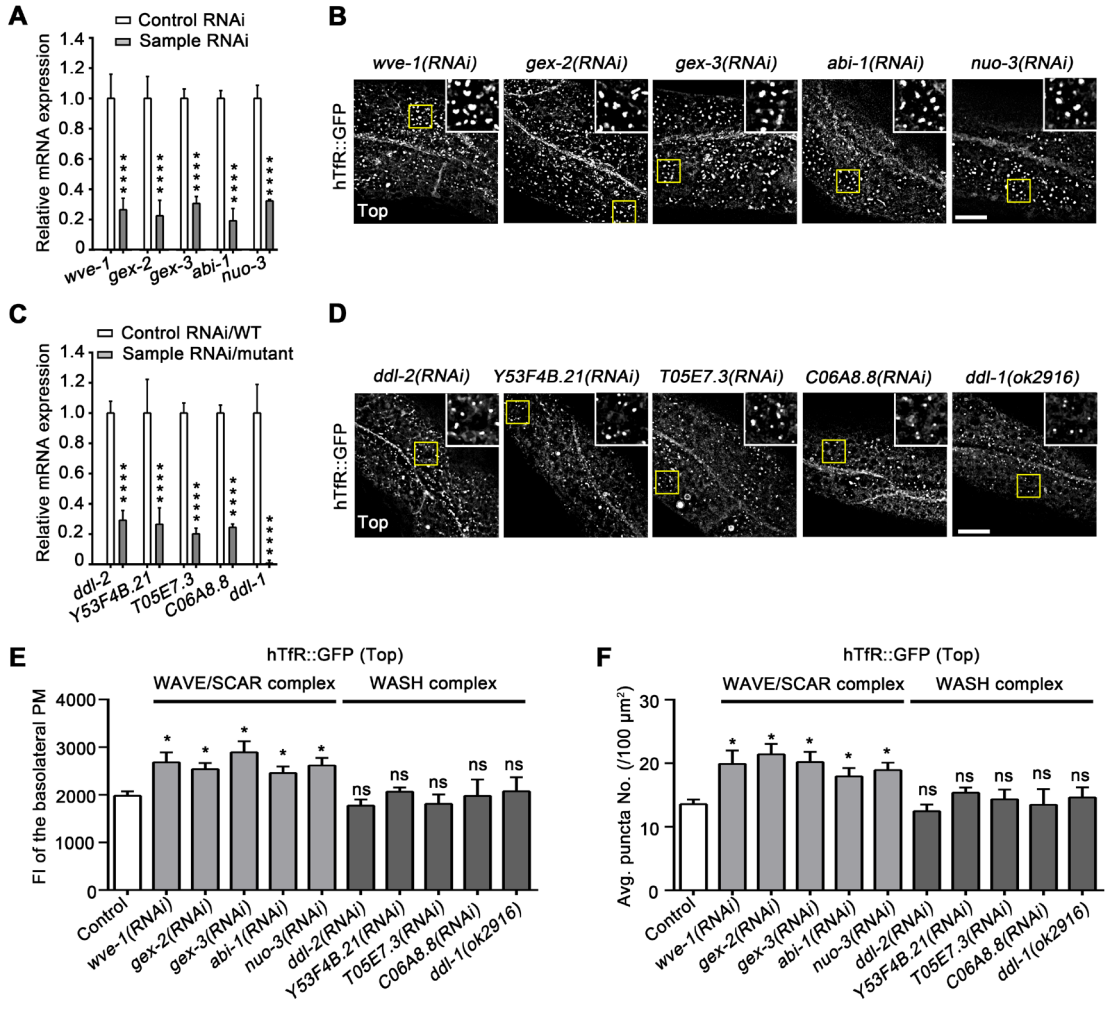

Fig. S2. Effect of disruption of WAVE/SCAR or WASH complex on the intestinal basal membrane-distributed hTfR::GFP. (A and C) qRT-PCR

quantification of the RNA silencing or knock-out efficiency for the individual WAVE/SCAR (A) or WASH (C) component genes. The mRNA levels in RNAi treatment animals were normalized to the levels in control animals, which were set as arbitrary unit 1. Data (mean±s.e.m.) were from three independent experiments. ****P<0.0001 (t-test). (B and D) Representative confocal images of hTfR::GFP at the intestinal basal membrane in worms depleting each component of the WAVE/SCAR (B) or WASH (D) complex. The insets are magnified view of the boxed areas. (E and F) Quantification of the average FI (E) and puncta number (F) of hTfR::GFP at the basal membrane depicted in B and D. n=20 regions from 20 animals were analyzed for each group. Data (mean±s.e.m.) were from three independent experiments. ns, not significant; *P<0.05 (one-way ANOVA). Scale bars: 10 µm.

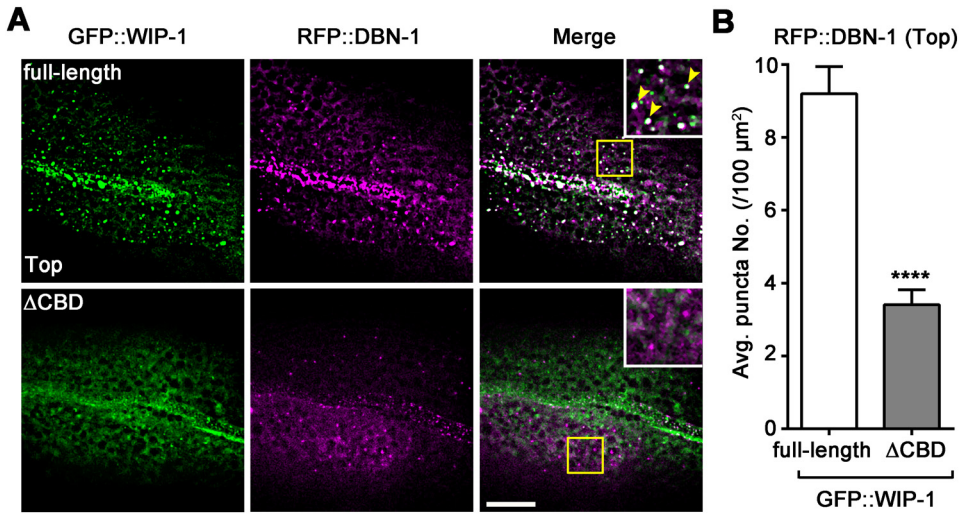

Fig. S3. CBD domain is essential for WIP-1 recruiting DBN-1 to CCPs. (A) Representative confocal images show the basal membrane localization of co-expressing GFP::WIP-1 full-length or ΔCBD construct with RFP::DBN-1. WIP-1 localization to the basal membrane was also influenced by the truncating deletion of CBD. Arrowheads indicate positive overlap. The insets are magnified view of the boxed areas. (B) The puncta number of RFP::DBN-1 per 100 µm^2 at the basal membrane were calculated for intestines depicted in A. n=20 regions from 20 animals were analyzed for

each group. Data (mean±s.e.m.) were from three independent experiments. ****P<0.0001 (Mann-Whitney). Scale bar: 10 µm.

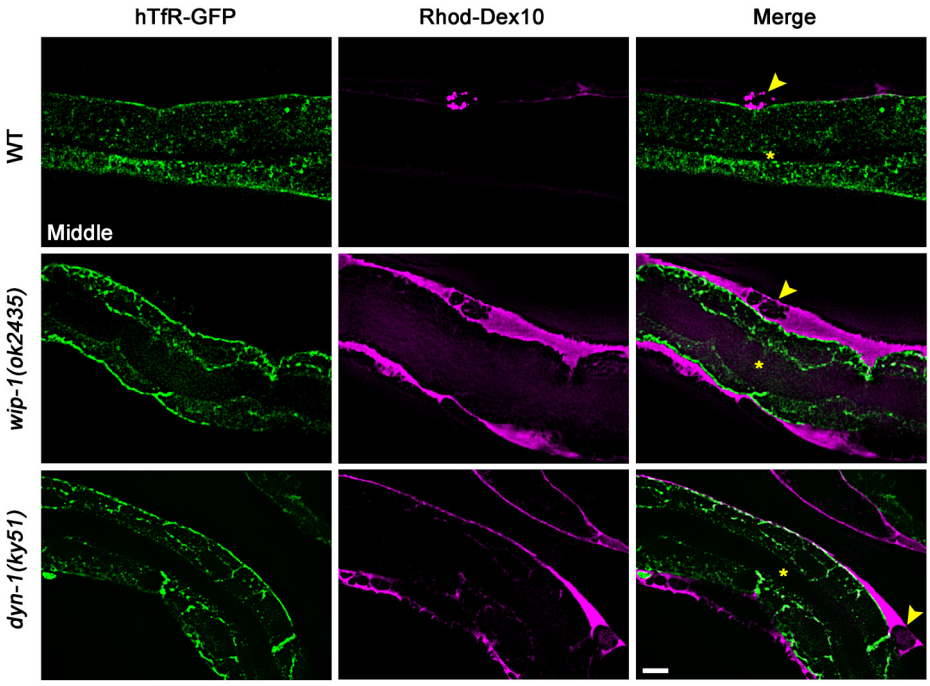

Fig. S4. Defective fluid-phase endocytosis of Rhod-Dex10 was induced in *wip-1(ok2435)* and *dyn-1(ky51)* mutants. Wild-type, *wip-1(ok2435)* and *dyn-1(ky51)* mutant intestines carrying hTfR::GFP exposed to basolateral Rhod-Dex10. Micrographs were taken 1 h after the Rhod-Dex10 injection into the pseudocoelom. The basolaterally internalized Rhod-Dex10 was fast-recycled out of the intestines back into the pseudocoelom and finally uptaken by the coelomocyte in wild-type animals, while in *wip-1(ok2435)* and *dyn-1(ky51)* mutant animals, Rhod-Dex10 was accumulated in the pseudocoeloms. Arrowheads point to coelomocytes, asterisks depict the lumen of the intestine. Scale bar: 10 µm.

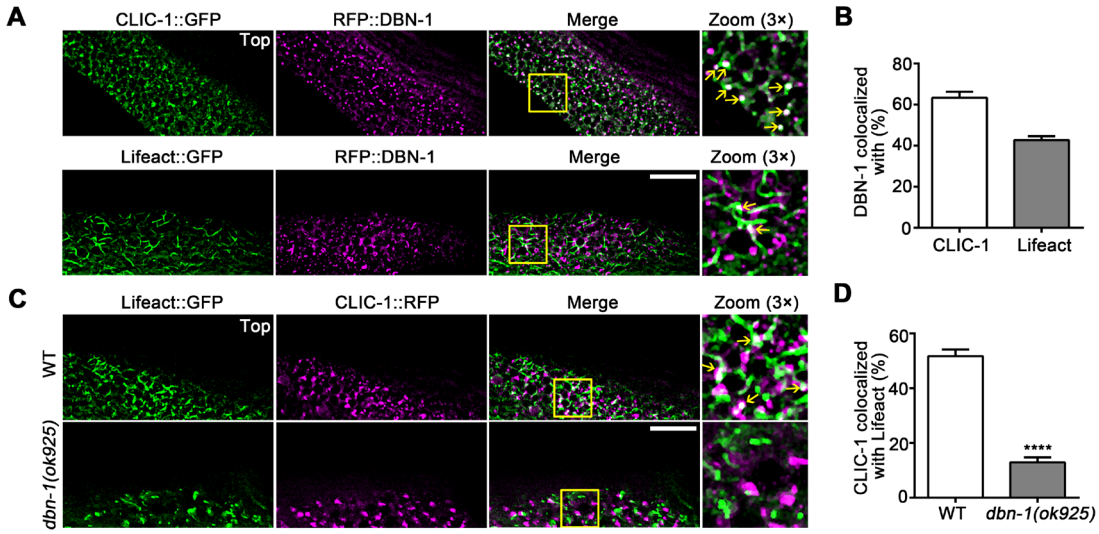

Fig. S5. DBN-1 promotes F-actin polymerization at the membrane-associated CCPs. (A and B) Representative colocalization images (A) and quantification (B) of RFP::DBN-1 with CLIC-1::GFP or Lifeact::GFP at the basal membrane. Insets show the enlargement of the indicated areas. Arrows indicate positive overlap. Note the decoration of DBN-1 on the tip or junction of Lifeact filaments. (C) Representative confocal images show the basal membrane localization of co-expressing Lifeact::GFP with CLIC-1::RFP in wild-type and *dbn-1(ok925)* mutants. Lifeact::GFP was obviously debranched and less colocalized with CLIC-1::RFP in *dbn-1* mutants. (D) Quantification of RFP-tagged CLIC-1 colocalized with Lifeact::GFP at the basal membrane for intestines of indicated genotypes. In B and D, *n*=15 regions from 12 animals for each group. Data (mean±s.e.m.) were from three independent experiments. ****P<0.0001 (Mann-Whitney). Scale bars: 10 µm.

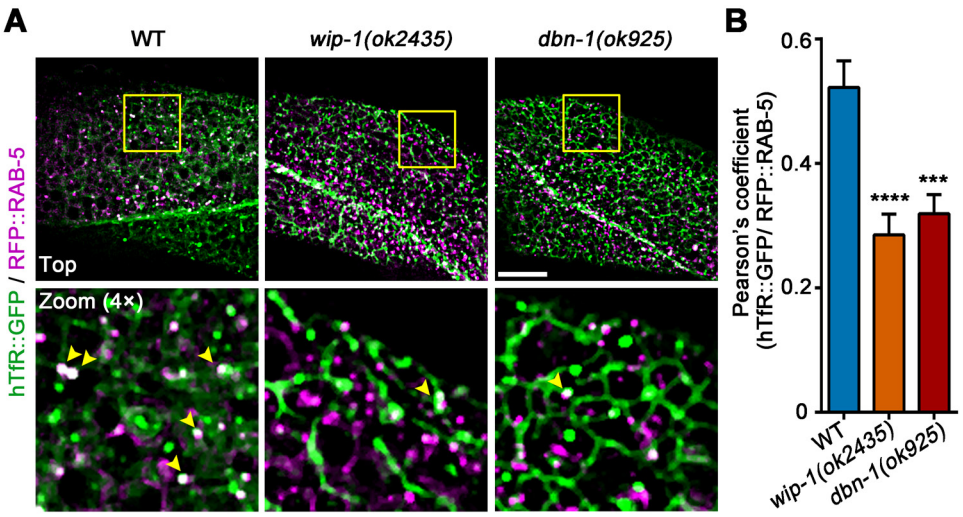

Fig. S6. The arrested hTfR-containing tubules caused by defective CCP scission are less labeled by RAB-5. (A) Colocalization images of hTfR::GFP with RFP::RAB-5 in wild-type, *wip-1(ok2435)* or *dbn-1(ok925)* mutant intestines. The Lower panels are enlargements of the outlined areas. Arrowheads indicate positive overlap. (B) Pearson's correlation coefficients for hTfR::GFP and RFP::RAB-5 signals depicted in A were calculated. *n*=20 regions from 20 animals for each genotype. Data (mean±s.e.m.) were from three independent experiments. ***P<0.001; ****P<0.0001 (one-way ANOVA). Scale bar: 10 µm.

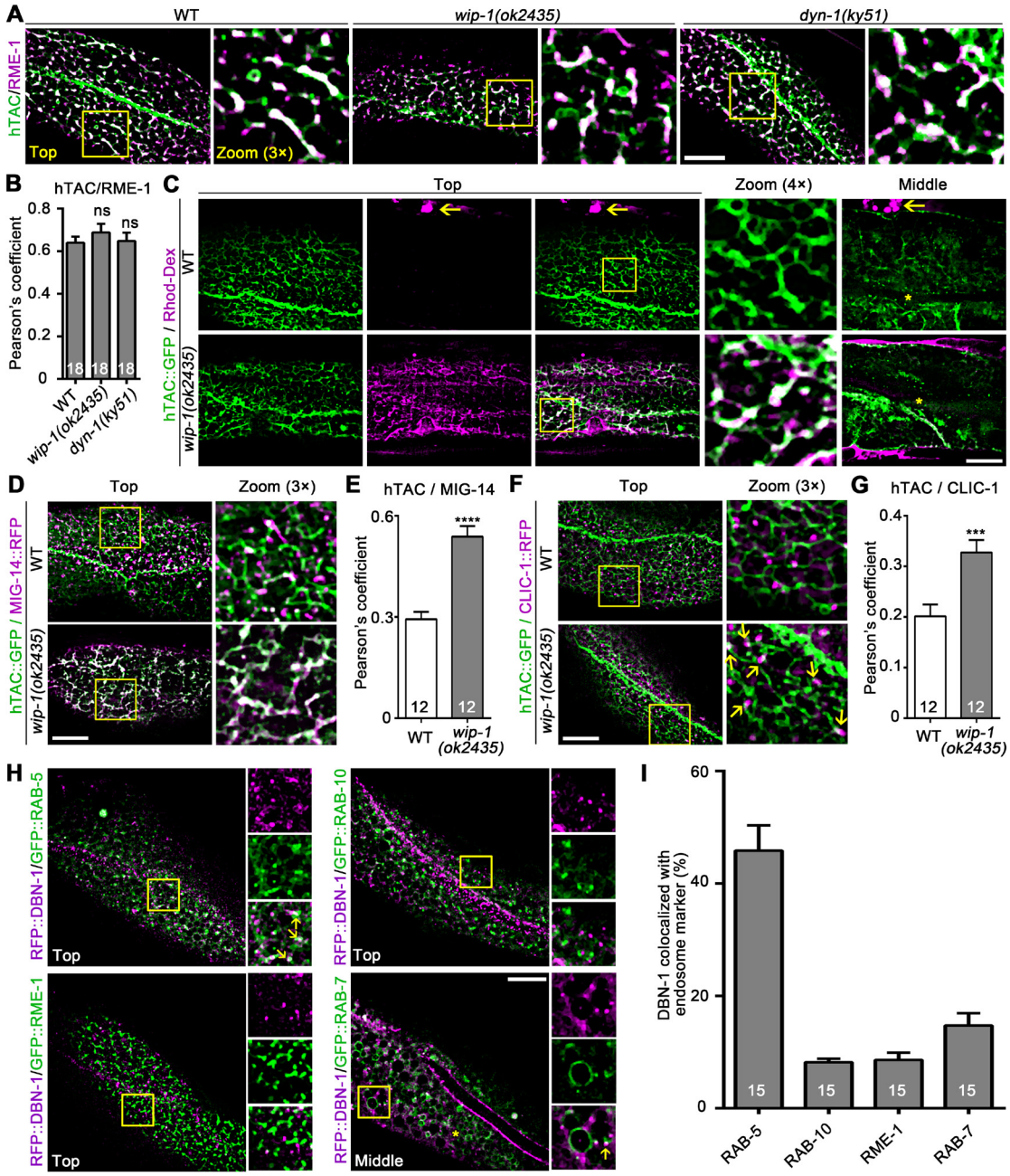

Fig. S7. WIP-1 also affects the internalization of hTAC in the intestine of *C. elegans*. (A) Colocalization images of hTAC::GFP with RFP::RME-1 in WT, *wip-1(ok2435)* and *dyn-1(ky51)* mutant intestines at 25°C. Insets are magnified view of the boxed areas. (B) Quantification of the colocalization by Pearson's colocalization coefficient. (C) Confocal images of basolaterally internalized Rhod-Dex10 in hTAC-GFP-expressing intestines of various mutants as indicated. Arrows indicate coelomocyte with internalized Rhod-Dex10. (D) Confocal images showing colocalization between

hTAC::GFP and MIG-14::RFP in the intestinal cells. hTAC tubules were extensively overlapped with the aberrant MIG-14 tubules in *wip-1* mutants. (E) Pearson's correlation coefficients for hTAC::GFP and MIG-14::RFP were calculated. (F) hTAC tubules were increasingly capped by clathrin in response to loss of WIP-1.(G) The levels of colocalization of hTAC::GFP and CLIC-1::RFP were determined by Pearson's correlation coefficients. (H and I) Representative colocalization images (H) and Quantification (I) of RFP::DBN-1 with GFP-tagged endosome markers in the intestine. Arrows indicate positive overlap. Asterisk depicts the intestine lumen. In B, E, G and I, the number of areas analyzed for each group is indicated in each bar. At least 12 animals were analyzed for each group. Data (mean±s.e.m.) were from three independent experiments. In B, ns, not significant (one-way ANOVA); In E and G, ****P<0.0001, ***P<0.001 (t-test). Scale bars: 10 μm.

Table S1. Mutant and transgenic strains used in this study.

Strain	**Genotype**
VC2053	*wip-1(ok2435) III* [a]
NG324	*wsp-1(gm324) IV* [a]
RB1004	*dbn-1(ok925) III* [a]
CX51	*dyn-1(ky51) X* [a]
VC2193	*ddl-1(ok2916) II* [a]
DH1201	*rme-1(b1045) V* [a]
tm2299	*wsp-1(tm2299) IV* [b]
RT1970	*unc-119(ed3) III; pwIs90[Pvha-6::hTfR::GFP, Cb-unc-119(+)]* [c]
RT2071	*unc-119(ed3) III; pwIs765[Pvha-6::MIG-14::GFP, Cb-unc-119(+)]* [c]
RT393	*unc-119(ed3) III; pwIs112[Pvha-6::hTAC::GFP, Cb-unc-119(+)]* [c]
RT548	*unc-119(ed3) III; pwIs216[Pvha-6::RFP::RME-1, Cb-unc-119(+)]* [c]
RT327	*unc-119(ed3) III; pwIs72[Pvha-6::GFP::RAB-5, Cbunc-119(+)]* [c]

RT525	*unc-119(ed3) III; pwIs206[Pvha-6::GFP::RAB-10, Cbunc-119(+)]* [c]
RT348	*unc-119(ed3) III; pwIs87[Pvha-6::GFP::RME-1, Cbunc-119(+)]* [c]
RT476	*unc-119(ed3) III; pwIs170[Pvha-6::GFP::RAB-7, Cbunc-119(+)]* [c]
RYZEx1	*[Pvha-6::TagRFP-T::WIP-1]* [d]
RYZEx2	*[Pvha-6::TagRFP-T::WIP-1(△1st WH2)]* [d]
RYZEx3	*[Pvha-6::TagRFP-T::WIP-1(△WBD)]* [d]
RYZEx4	*[Pvha-6::TagRFP-T::WIP-1(△CBD)]* [d]
RYZEx5	*[Pvha-6::GFP::WIP-1]* [d]
RYZEx6	*[Pvha-6::DYN-1::TagRFP-T]* [d]
RYZEx7	*[Pvha-6::DYN-1::GFP]* [d]
RYZEx8	*[Pvha-6::ARX-2::TagRFP-T]* [d]
RYZEx9	*[Pvha-6::TagRFP-T::DBN-1]* [d]
RYZEx10	*[Pvha-6::TagRFP-T::DBN-1(△ADF-H)]* [d]
RYZEx11	*[Pvha-6::TagRFP-T::DBN-1(△3CC)]* [d]
RYZEx12	*[Pvha-6::TagRFP-T::DBN-1(△PRD)]* [d]
RYZEx13	*[Pvha-6::TagRFP-T::DBN-1(△SH3)]* [d]
RYZEx14	*[Pvha-6::GFP::WIP-1(△CBD)]* [d]
RYZEx15	*[Pvha-6::CLIC-1::TagRFP-T]* [d]
RYZEx16	*[Pvha-6::CLIC-1::GFP]* [d]
RYZEx17	*[Pvha-6::Lifeact::GFP]* [d]
txuEx14	*[Pvha-6::TagRFP-T::RAB-5]* [d]

a. These mutant strains were provided by the *Caenorhabditis* Genetics Center (University of Minnesota, Minneapolis, MN). b. This strain was provided by the National BioResource Project (Tokyo Women's Medical University, Tokyo, Japan). c. These integrated transgenic strains were gifts from Professor Barth D. Grant (Rutgers University, Piscataway, NJ, USA). d. These extrachromosomal transgenic strains were obtained by using standard microinjection techniques.

Table S2. The specific primers used in Real-Time PCR analysis.

Gene	Primer	Oligo (5'-3')
wip-1	Forward	ACCATCCAGCAATGCTCGAAATG
	Reverse	CCATTTCCGTTTCCAGAATTTCC
wve-1	Forward	GCTTCAATGTACTGCTAATGGGAC
	Reverse	GTGATTTATTATCATTGCGTCGTG
gex-2	Forward	CTCTACAATGATGCTGCACAATACTCG
	Reverse	TCGAGAAGCATACACGACGCGAGCTG
gex-3	Forward	GTTAAAATTGGAGAAATGTCAGC
	Reverse	CAATTCGTGGAATACAGATAGCG
abi-1	Forward	GCGTAGCCTACCAGATTAACAAG
	Reverse	AATTTCTCGTCTTGCAAGCTTCTC
nuo-3	Forward	CCGCTTATAAGGAGTTCCAACG
	Reverse	TGAGTTTCTCCGACAAGTCTGTC
ddl-2	Forward	GAAGGGGAAATTCGATGGGATTC
	Reverse	CACTTTCCCATTGATCGCCTTCC
Y53F4B.21	Forward	GAAGGTCTACACCCGTATGCAACAG
	Reverse	GAAATAGCAGTAATTTGTCACG
T05E7.3	Forward	TGAAAGCTCTCTGAGTTGGAAAG
	Reverse	GTGCATTAGATATGTACTCAATC
C06A8.8	Forward	TCTCGTATGTCAGAGTTTAACAAC
	Reverse	CCCTTTCAGTGCATCTTCTCTTTC
ddl-1	Forward	TTTGATAAGAACCGTCGTAG
	Reverse	TGATGGAATCGAAATTGGCAGG
arx-2	Forward	TAAGGATTTGATGGTTGGCGAGG
	Reverse	TGCGCCATATCATCCCAGTTTC
chc-1	Forward	CAACGAGGCTTTGAATCAGTTGC
	Reverse	GCTTCCATCTGTTGTTTCCCTTG
wsp-1	Forward	TGGATCATGGTTCCGGAAAG

	Reverse	TATTCGAGAATCCACTATCC
tba-1	Forward	TGCTTGCTGGGAGCTCTACTGTCTC
	Reverse	CAACAACAGTTGGCTCAAGATCTAC